ORIGINAL ARTICLE

"Help is in the air": volatiles from salt-stressed plants increase the reproductive success of receivers under salinity

Marco Landi[1,2] · Fabrizio Araniti[3] · Guido Flamini[4] · Ermes Lo Piccolo[1] · Alice Trivellini[5] · Maria Rosa Abenavoli[3] · Lucia Guidi[1,2]

Abstract

Main conclusion Salinity alters VOC profile in emitter sweet basil plants. Airborne signals by emitter plants promote earlier flowering of receivers and increase their reproductive success under salinity.

Abstract Airborne signals can prime neighboring plants against pathogen and/or herbivore attacks, whilst little is known about the possibility that volatile organic compounds (VOCs) emitted by stressed plants alert neighboring plants against abiotic stressors. Salt stress (50 mM NaCl) was imposed on *Ocimum basilicum* L. plants (emitters, namely NaCl), and a putative alerting-priming interaction was tested on neighboring basil plants (receivers, namely NaCl-S). Compared with the receivers, the NaCl plants exhibited reduced biomass, lower photosynthesis, and changes in the VOC profile, which are common early responses of plants to salinity. In contrast, NaCl-S plants had physiological parameters similar to those of nonsalted plants (C), but exhibited a different VOC fingerprint, which overlapped, for most compounds, with that of emitters. NaCl-S plants exposed later to NaCl treatment (namely NaCl-S + NaCl) exhibited changes in the VOC profile, earlier plant senescence, earlier flowering, and higher seed yield than C + NaCl plants. This experiment offers the evidence that (1) NaCl-triggered VOCs promote metabolic changes in NaCl-S plants, which, finally, increase reproductive success and (2) the differences in VOC profiles observed between emitters and receivers subjected to salinity raise the question whether the receivers are able to "propagate" the warning signal triggered by VOCs in neighboring companions.

Keywords Airborne signal · Emitter · Infochemical · Plant–plant communication · Receiver · Salt stress

Abbreviations

A_N	Net photosynthesis
$F_0/F_m/F_v$	Minimal/maximal/variable chlorophyll fluorescence yield in dark-adapted leaves

✉ Marco Landi
marco.landi@unipi.it

Fabrizio Araniti
fabrizio.araniti@unirc.it

Guido Flamini
guido.flamini@farm.unipi.it

Ermes Lo Piccolo
ermes.lopiccolo@gmail.com

Alice Trivellini
alice.trivellini@gmail.com

Maria Rosa Abenavoli
mrabenavoli@unirc.it

Lucia Guidi
lucia.guidi@unipi.it

[1] Department of Agriculture, Food and Environment, University of Pisa, Via del Borghetto 80, 56124 Pisa, Italy

[2] CIRSEC, Centre for Climatic Change Impact, University of Pisa, Via del Borghetto 80, 56124 Pisa, Italy

[3] Department of Agraria, University 'Mediterranea' of Reggio Calabria, località Feo di Vito, 89122 Reggio Calabria, RC, Italy

[4] Department of Pharmacy, University of Pisa, Via Bonanno Pisano 6, 56126 Pisa, Italy

[5] Institute of Life Sciences, Scuola Superiore Sant'Anna, Via Santa Cecilia 3, 56127 Pisa, Italy

g_s Stomatal conductance
PCA   Principal component analyses
VOC   Volatile organic compound
WUE   Water use efficiency

Introduction

Sessility in plants exposes them, for most of their life, to adverse biotic and abiotic stresses; however, they are able to evade stressful events because of their extraordinary plasticity to perceive and respond to fluctuating or drastic environmental cues (Covarrubias et al. 2017). Plants are peerless "masters" of gas exchange; they not only build 10-m-high trees simply from CO_2 taken up from the air but also invest a considerable amount of freshly assimilated carbon into volatile organic compounds (VOCs), which are released back into the atmosphere (Loreto et al. 2014). Several studies have confirmed that VOC emission is not a mere waste of assimilated carbon, but it serves several ecological functions including attraction of pollinators, scavenging of reactive oxygen species, and tolerance to high temperature or atmospheric pollution, plant defense against herbivores and pathogens (for a review see Yuan et al. 2009; Loreto et al. 2014; Ameye et al. 2017; Fincheira and Quiroz 2018). From the first milestone on "talking trees" (Baldwin and Schultz 1983), it has been extensively elucidated that VOCs can serve as infochemicals in the communication between plants (Guerrieri 2016).

A conspicuous body of research deals with plant–plant communication stimulated by biotic factors. For example, VOCs emitted by plants could affect plant communities, and when plants are attacked by herbivores or pathogens (emitters), the signals by the emitter plants can be "eavesdropped" by the neighboring plants (receivers), thus warning and alerting receivers for possible future attacks (Yoneya and Takabayashi 2014). Although abiotic stressors (including salinity, drought, high temperature, metal toxicity, and ultraviolet radiation) can also reasonably alter the fingerprint of infochemical VOCs emitted by plants (Loreto et al. 2014; Forieri et al. 2016; Ameye et al. 2017), thereby altering mutualistic relationships and plant competition promoted by VOC emission (Kegge and Pierik 2010), scarce information is available on plant–plant communication triggered by abiotic factors (e.g., Bibbiani et al. 2018; Catola et al. 2018). Regarding plant–plant communication under salt stress conditions, available studies (Lee and Seo 2014; Caparrotta et al. 2018) have revealed that changes in the VOC profile by emitter plants triggered reactive reactions in receivers, which enabled receivers to better cope with salinity. Lee and Seo (2014) observed that the receiver plants of *Arabidopsis* were more tolerant than emitters grown with 150 mM NaCl, suggesting that salt-promoted changes in VOCs are relevant in priming salt tolerance in neighboring plants and observed that emission of VOCs was dependent on NaCl doses. Caparrotta et al. (2018) demonstrated that the receiver plants of *Vicia faba* maintained a higher photosynthetic rate, photosystem II (PSII) efficiency, and relative growth rate than emitters when subsequently subjected to salt stress. The authors hypothesized that leaf volatiles, methanol, and terpenes can act as airborne signals in salt stress communication. Jalali et al. (2017) observed that VOC emitted by *Trichoderma* spp. increase growth and induce salt tolerance in *Arabidopsis thaliana*.

To the best of our knowledge, information on the influence of VOC produced by emitters under salt stress on the reproductive success of receivers when subjected to the same stress is lacking. In addition, no studies have investigated whether the VOC fingerprint differs in emitters and receivers when subjected to salt stress, which would clarify the (im)possibility by receivers to "propagate" the warning signal triggered by the emitters of VOCs. To fill this knowledge gap, with the present set of experiments, we investigated in sweet basil plants whether salinity promoted changes in the volatilome of emitter plants, thus alerting neighboring receivers and eliciting their subsequent response to salt stress. We employed gas exchange, chlorophyll fluorescence, pigment composition, and targeted metabolomic analyses to assess the effect of volatile cues produced by emitters on the physiological performances of nearby unstressed plants. We also compared plant reproductive success (in terms of seed production and germination rate) of salt-stressed emitters and receivers.

Materials and methods

Plant material and growth conditions

Experimental activities were conducted in the spring of 2018 at the Department of Agriculture, Food and Environment—University of Pisa (43° 43′ 00″ N 10° 24′ 00″ E, Pisa, Italy). The seeds of green basil (*Ocimum basilicum* L.) cv. "Tigullio" were purchased from Franchi Sementi Spa (Bergamo, Italy). After germination, seedlings were grown for 2 weeks in a hydroponic floating system to ensure plant uniformity, as described in Pardossi et al. (2015). The seedlings were then transferred in 2-L pots filled with a sandy soil-peat mixture (60:40, v:v). The plants were irrigated daily with an excess of a nutrient solution optimized for sweet basil cultivation (Landi et al. 2013) to avoid mineral accumulation in the substrate and minimize the differences in micronutrient and/or macronutrient concentration, which can occur between the feeding solution and the growing media. Salt treatment was provided by adding 50 mM NaCl to the aforementioned solution. During the experiments, the minimum

and mean ventilation air temperatures were 13.2 °C and 26.5 °C, respectively. The maximum temperature reached 35 °C and the mean values of daily air temperature and global solar radiation were 22.7 °C and 11.6 MJ m^{-2} day^{-1}, respectively. During the greenhouse experiments (steps 1 and 2, see below), the plants were maintained in 1-m^3 plastic boxes (1 m × 1 m × 1 m; 20 plants each). The boxes had a 2-cm hole (ø) positioned near each corner of the upper face, which avoided the confounding effect attributable to different evapotranspiration between controls and salt-treated plants (by equilibrating the internal conditions of each box to those of the greenhouse) and, at the same time, avoided communication by plants located in different boxes.
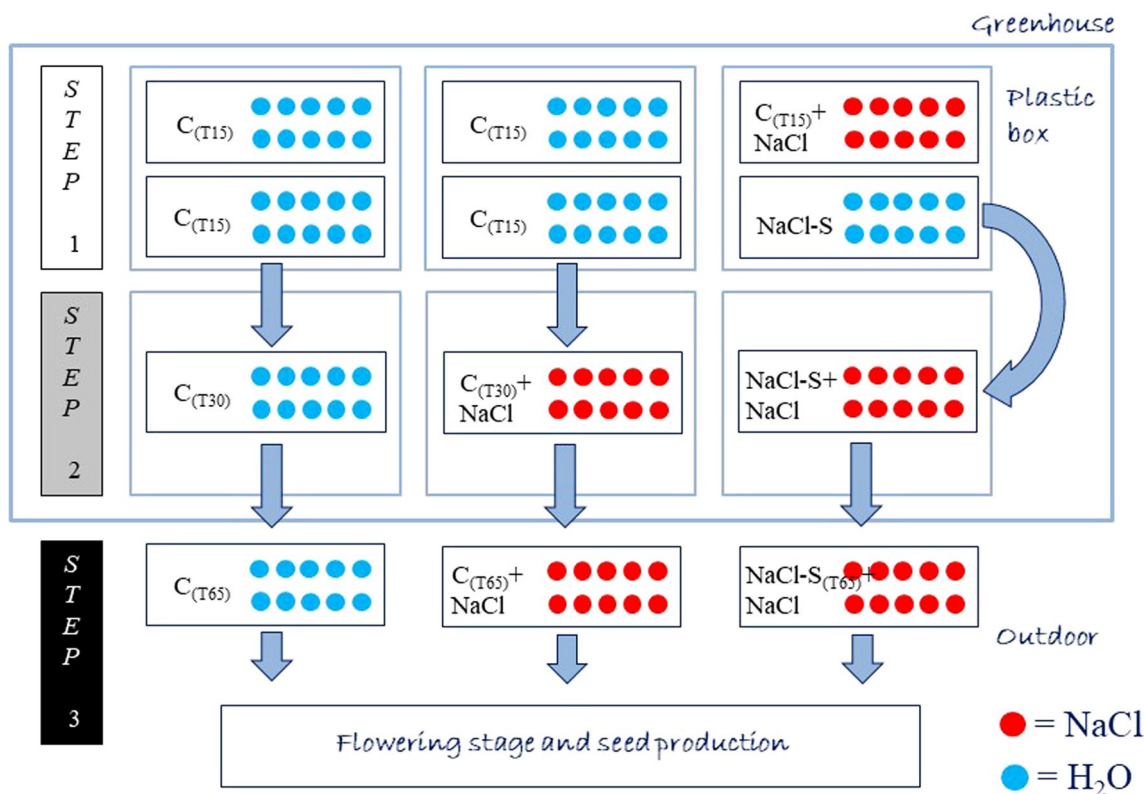
Experimental design

To test our hypothesis, the whole experiment was temporally divided into three subsequent steps (Fig. 1). In step 1, 10 plants of sweet basil were treated with 50 mM NaCl for 15 days [emitters; $C_{(T15)}$ + NaCl] whereas other 10 unstressed plants where placed together with emitters, but irrigated with water without NaCl (receivers; namely NaCl-smelling plants; NaCl-S). During the 15 days of salt treatment, the plants were positioned inside each box as shown in Fig. 1 and their position was changed daily to minimize the possible effects of the plant position. Each plant has a distance of 10 cm from their relative neighboring plants. Other 40 plants, namely $C_{(T15)}$ (20 for each box; 2 boxes) were grown as controls and irrigated without the addition of NaCl, as similarly to NaCl-S plants.

In step 2, 10 $C_{(T15)}$ plants were maintained as controls for further 15 days (10 plants, namely C_{T30}), while other 10 $C_{(T15)}$ plants [$C_{(T30)}$ + NaCl] and 10 NaCl-S receiver plants (NaCl-S + NaCl) were given 15 days of 100 mM NaCl. This step allowed us to establish the response of emitters and receivers to salinity. All plants in step 2 have the same age (T30).

In step 3, plants were placed outdoor to allow pollination. Plants belonging to specific treatment were separated from each other to avoid cross-influence of VOC emission. Treatments were prolonged for further 35 days until when $C_{(T65)}$ + NaCl plants started developing the first floral

Fig. 1 Experimental design employed to test plant–plant communication. Step 1: $C_{(T15)}$ represents control plants, $C_{(T15)}$ + NaCl represents the plants treated with 50 mM NaCl for 15 days and NaCl-S represents the control plants exposed for 15 days to airborne signals emitted by $C_{(T15)}$ + NaCl plants. Step 2: after 15 days, NaCl-S plants were treated with 50 mM NaCl, similar to control plants of the same age, which were not previously exposed to volatiles, namely $C_{(T30)}$ + NaCl.

Plants that were not previously exposed to volatiles and irrigated with water were used as controls, namely $C_{(T30)}$. Step 3: plants were placed outdoor to allow pollination and the treatment described in step 2 was protracted until the flowering stage and seed production. After 35 days from the beginning of step 2 (T65), some plants were collected for determination of total C, Na$^+$, and Cl$^-$ accumulation

primordium, NaCl-S$_{(T65)}$ + NaCl plants were in an advanced flowering stage, and C$_{(T65)}$ plants had no floral primordium. This step allowed us to monitor the difference in plant ontogenesis among the treatments.

Then, plants belonging to each treatment were allowed to flower and produce seeds. The seeds were collected at maturity, kept in the dark at 4 °C for 15 days to overcome vernalization, and then the percentage of germination was calculated as reported by Ceccanti et al. (2018).

Biomass, total C, total N, Na$^+$, and Cl$^-$ determination

In the plants from steps 1 and 2, the leaves and shoots were separated and their fresh weight (FW) was recorded. For dry weight (DW) determinations, both the leaves and shoots were dried at 70 °C until a constant weight was reached. In plants from step 3, leaf tissue nitrogen was determined in triplicate by the Kjeldahl method (Jones 1998), whereas total carbon was determined as described in Sims and Kline (1991). Na$^+$ and Cl$^-$ concentrations were quantified as described in Pompeiano et al. (2017).

Gas exchange and chlorophyll fluorescence

Gas exchange parameters, i.e., photosynthetic rate (A_N; μmol CO$_2$ m^{-2} s^{-1}), intercellular CO$_2$ concentration (C_i; μmol CO$_2$ mol air^{-1}), stomatal conductance (g_s; mol H$_2$O m^{-2} s^{-1}), and intrinsic water use efficiency [WUE = A_N/g_s; (μmol CO$_2$ mol H$_2$O^{-1}) were measured in top fully expanded leaves (one leaf per plant; five plants per treatment) using a Portable Infrared Gas Analyzer (Li-6400; LI-COR Inc., Lincoln, NE, USA). To avoid the effects of fluctuating environmental conditions on gas exchange parameters, the measurements were performed in the morning (10.30 am to 12.00 a.m.; solar time) in light-saturated light conditions (1200 μmol photons m^{-2} s^{-1}) and at an ambient CO$_2$ concentration (400 ± 5 μmol CO$_2$ mol air^{-1}), while leaf temperature ranged between 26.2 and 28.4 °C.

Chlorophyll fluorescence parameters were measured in dark-adapted leaves, homogeneous to the leaves used for gas exchange, using a PAM–2000 chlorophyll fluorometer (Walz, Effeltrich, Germany). The maximum efficiency of PSII photochemistry was calculated as follows: $F_v/F_m = (F_m—F_0)/F_m$, where F_v is the variable fluorescence, and F_m and F_0 are the maximum and minimal fluorescence yield in (30 min) dark-adapted leaves before and after a saturating pulse (8000 μmol m^{-2} s^{-1} for 1 s), respectively.

Chlorophyll and carotenoid determinations

Chlorophylls and carotenoids were extracted as described by Papadakis et al. (2018). Chlorophyll and carotenoid concentrations were determined spectrophotometrically by collecting extract absorbance at 470 nm, 647 nm, and 663 nm and using the equations described by Lichtenthaler and Buschmann (2001).

Flavonoid index

Flavonoid index was estimated using a Dualex Scientific optical sensor (Force-A, Centre Universitaire Paris Sud, France), which measures the leaf epidermal absorbance at 520 nm using the chlorophyll fluorescence screening method (Agati et al. 2011), equalizing the chlorophyll fluorescence signal under the 520 nm excitation and that under red excitation at 650 nm, as reported in Goulas et al. (2004).

Ethylene determination

Ethylene production was measured by enclosing leaves in 90-mL air-tight containers, 15 min after excision to avoid ethylene production effects of wounding. Of the gas samples, 2 mL was taken from the headspace of the containers after 1 h of incubation at room temperature. Ethylene concentration in the samples was measured by a gas chromatograph (HP5890, Hewlett-Packard, Menlo Park, CA, USA) using a flame ionization detector, a stainless steel column (150 × 0.4 cm ø packed with HayeSep$^®$ Porous Polymer Adsorbent; Sigma-Aldrich, Milan, Italy), and the column and detector temperatures were 70 °C and 350 °C, respectively, and nitrogen was used the carrier gas at a flow rate of 30 mL min^{-1}. Quantification was performed against an external standard and results were expressed on an FW basis (nL g^{-1} FW h^{-1}). To ensure sample representativeness, each independent biological replicate (in total $n = 4$) was created by pooling together three different leaves from the same plants, collected at three different positions of the plant stem (i.e., different developmental stage).

Solid phase microextraction and analysis

For headspace-solid phase microextraction (SPME), Supelco SPME devices coated with polydimethylsiloxane (100 μm; Sigma-Aldrich) were used. Fully expanded undamaged leaves were collected all around the plants, immediately inserted into a 100-mL glass conical flask, allowed to equilibrate for 20 min, and then exposed to the headspace for 15 min at room temperature. Once sampling was finished, the fiber was withdrawn into the needle and transferred to the injection port of the gas chromatography-mass spectrometry (GC–MS) system.

GC–MS analyses were performed with a gas chromatograph (CP-3800, Varian, Palo Alto, CA, USA) equipped with an HP-5 capillary column (30 m × 0.25 mm; coating thickness, 0.25 μm) and an ion-trap mass detector (Saturn 2000, Varian). Injector and transfer line temperatures were

220 °C and 240 °C, respectively. The oven temperature was programmed from 60 to 240 °C at 3 °C min^{-1} ramp, with helium as the carrier gas (flow rate 1 mL min^{-1}) in the split-less injection mode. The constituents were identified by comparing the retention times with those of the standard samples and their linear retention indices relative to a series of *n*-hydrocarbons were matched against a commercial (NIST 2014 and ADAMS) and home-made library of mass spectra built up from pure substances and components of known essential oils and the literature data on MS (Adams 1995). Quantitative comparisons of relative peaks areas (%) were performed between the same chemicals in the different samples.

Metabolome extraction, derivatization, and GC–MS analysis

Plant material was extracted and derivatized as previously reported by Araniti et al. (2017) with few modifications. Lyophilized plant material (10 mg), for each sample and replicates, was transferred into 2-mL screw cap tubes. Plant material was extracted adding 1400 μL of 100% methanol (− 20 °C) and 60 μL of ribitol (internal quantitative standard 0.2 mg mL^{-1} in dH$_2$O) was added and vortexed for 10 s. The samples were transferred in a thermomixer at 70 °C and shaken for 10 min (950 rpm) and then centrifuged for 10 min at 11,000g. The supernatants were collected and transferred to a glass vial, where 750 μL of CHCl$_3$ and 1500 μL of dH$_2$O were added. All samples were vortexed for 10 s and then centrifuged for 15 min at 2200g. For each sample and replicate, an aliquot of 115 μL from the polar phase was collected, transferred to a 1.5-mL tube, and vacuum concentrated.

Derivatization was performed by adding 40 μL of methoxyamine hydrochloride (20 mg mL^{-1} in pyridine) followed by a 2-h incubation in a thermomixer (950 rpm) at 37 °C. Methoxyamine hydrochloride-treated samples were then silylated by adding 70 μL of *N*-methyl-*N*-(trimethylsilyl)trifluoroacetamide to the aliquots and incubating for 30 min at 37 °C. The derivatized extracts were injected into a TG-5MS capillary column using a gas chromatograph apparatus (Trace 1310, Thermo Fisher, Waltham, MA, USA) equipped with a single quadrupole mass spectrometer. Injector and source were set at 250 °C and 260 °C, respectively. The sample (1 μL) was injected in the split-less mode at a flow rate of 1 mL min^{-1} using the following programmed temperatures: isothermal 5 min at 70 °C followed by a 5 °C min^{-1} ramp to 350 °C and a final 5-min heating at 330 °C. Mass spectra were recorded in electronic impact (EI) mode at 70 eV, scanning at 45–500 *m/z* range. The mass spectrometric solvent delay was set as 9 min.

Statistical analyses

The experiment was set up following a completely-randomized experimental design. All data were subjected to Bartlett's test to assess the homoscedasticity of the data across populations. For each experimental step, data were subjected to one-way analysis of variance (ANOVA) with salinity as the variability factor and then the means were separated with Fisher's least significant difference (LSD) post hoc test ($P \leq 0.05$). The percentage values were angularly transformed before the analyses. All statistical analyses were performed using GraphPad (GraphPad, La Jolla, CA, USA).

Metabolomic data were analyzed using Metaboanalyst 3.0 (https://www.metaboanalyst.ca/) (Xia et al. 2015). The data, expressed as metabolite concentrations, were checked for integrity and missing values were ascribed to the molecules with low-intensity signal and replaced with a small positive value (the half of the minimum positive values in the original data) assumed to be the detection limit. The data were successively normalized by the pre-added internal standard (ribitol), transformed through "Log normalization," and scaled through Pareto Scaling. The data were then classified through Principal Component Analysis (PCA) and metabolite variations were presented as a heat map.

Results

Plant biomass

In step 1, the salt treatment caused shoot biomass reduction (see C$_{(T15)}$ + NaCl in Fig. 2a, b), whereas both control and receiver plants had similar values of shoot biomass. In step 2, both types of NaCl-treated plants had reduced shoot biomass compared with the controls, but notably, the receivers, NaCl-S + NaCl, had more reduced shoot biomass compared with C$_{(T30)}$ + NaCl plants (Fig. 2a, b).

## Gas exchange and chlorophyll fluorescence

In step 1, the values of A_N were similar in the plants irrespective of the treatment (Fig. 3a). Conversely, the salt-treated plants, C$_{(T15)}$ + NaCl, had constrained g_s (Fig. 3b), reduced intercellular CO$_2$ concentration (C_i; Fig. 3c), and higher values of WUE (Fig. 3d), which are typical plant stress responses to salinity. Compared with the controls, C$_{(T15)}$, NaCl-S plants did not differ in gas exchange parameters, except for the slightly (but significant) higher level of WUE. The salt-treated plants in step 1 did not undergo photoinhibition (Fig. 3e), but they had a strong increase in F_0 (Fig. 3f). In step 2, when receivers were supplied with NaCl (NaCl-S + NaCl), they showed the strongest decrease in A_N and g_s, together with the highest values of WUE (Fig. 3a,
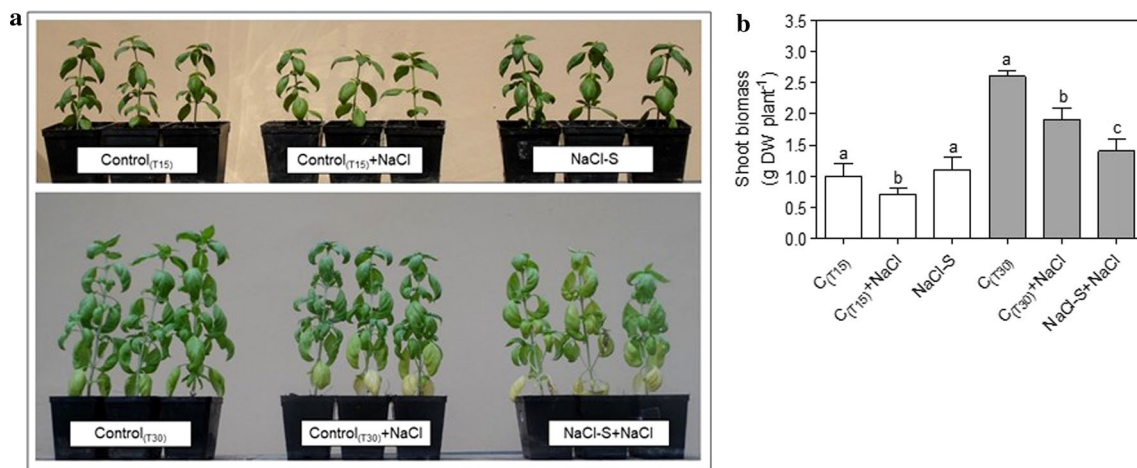
Fig. 2 **a** Plant phenotype and **b** shoot biomass production of sweet basil (*Ocimum basilicum* L.) plants irrigated without the addition of NaCl for 15 [$C_{(T15)}$] or 30 days [$C_{(T30)}$], irrigated with 50 mM NaCl for 15 [$C_{(T15)}$+NaCl] or 30 days [$C_{(T30)}$+NaCl], irrigated without NaCl and grown together with $C_{(T15)}$+NaCl plants (NaCl-S), and NaCl-S plants further irrigated with 50 mM NaCl for 15 days (NaCl-S+NaCl). In **b**, data (means±SD, $n=3$) were subjected to one-way ANOVA, and bars not accompanied by the same letter in step 1 (white bars) or step 2 (grey bars) are significantly different at $P \leq 0.05$ after LSD test

Fig. 3 **a** Net photosynthesis (A_N), **b** stomatal conductance (g_s), **c** intercellular CO_2 concentration (C_i), **d** intrinsic water use efficiency (WUE=A_N/g_s), **e** maximal PSII efficiency for photochemistry (F_v/F_m), and **f** minimum fluorescence yield of PSII in dark-adapted state (F_0) in the leaves of sweet basil (*Ocimum basilicum* L.) plants irrigated without the addition of NaCl for 15 [$C_{(T15)}$] or 30 days [$C_{(T30)}$], irrigated with 50 mM NaCl for 15 [$C_{(T15)}$+NaCl] or 30 days [$C_{(T30)}$+NaCl], irrigated without NaCl and grown together with $C_{(T15)}$+NaCl plants (NaCl-S), and NaCl-S plants further irrigated with 50 mM NaCl for 15 days (NaCl-S+NaCl). Data (means±SD, $n=5$) were subjected to one-way ANOVA and bars not accompanied by the same letter in step 1 (white bars) or step 2 (grey bars) are significantly different at $P \leq 0.05$ after LSD test
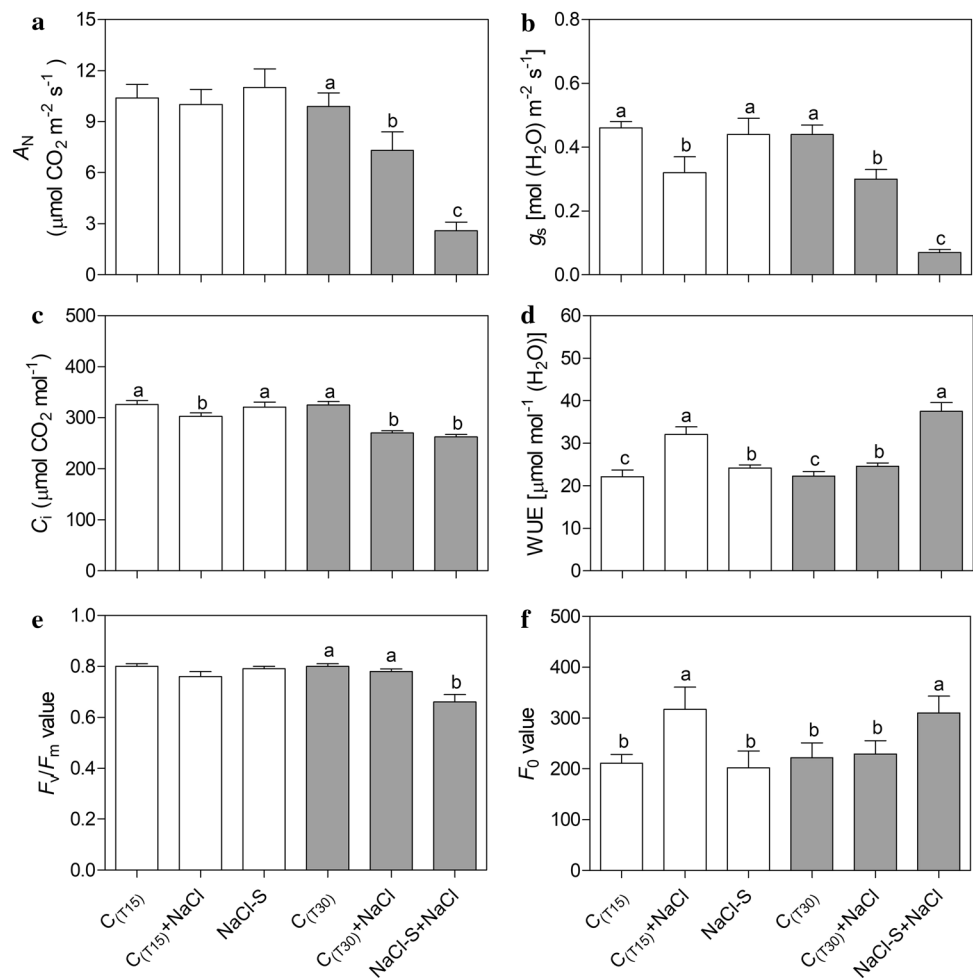
b, d, respectively). In addition, NaCl-S + NaCl were the only plants that underwent photoinhibition and in which an increase in F_0 was observed (Fig. 3e, f). Although the effect of 50 mM NaCl was less severe in $C_{(T30)}$ + NaCl plants than in salt-treated receivers, values of A_N and g_s were also impaired in $C_{(T30)}$ + NaCl plants compared with controls, with a slight increase in WUE (Fig. 3a, b, d, respectively).

Photosynthetic pigment content and flavonoid index

In step 1, neither emitters nor receivers showed significant differences in pigment composition and flavonoid index compared with $C_{(T30)}$ plants (Fig. 4a–f). In step 2, salt stress-induced slight changes in the pigment composition in $C_{(T30)}$ + NaCl plants, including a reduction in the chlorophyll (Chl) *a/b* ratio and an increase in total carotenoid content, were observed. On the other hand, the stress provoked severe modification in the pigment composition and flavonoid index in salt-treated receiver plants (NaCl-S + NaCl). The Chl *a* + *b* level was reduced by about 50% (Fig. 4c) in

$C_{(T30)}$ plants, and the reduction was attributable to the loss of both Chl *a* and *b* (Fig. 4a, f, respectively). This effect was associated with a steep increase in the Car tot concentration (Fig. 4e) and flavonoid index (Fig. 4f).

Metabolomic profile

To understand the modulation of metabolic homeostasis caused by the different treatments, untargeted GC–MS analysis was performed and the results are presented in Fig. 5a–d and Table S1. This analysis allowed us to identify differentially produced metabolites among all treatments. Sixty-four metabolites, including 9 amino acids, 17 organic acids, 2 phenolic acids, 18 sugars, 6 sugar alcohols, 1 amine, 4 fatty acids, 1 alkaloid, and 5 miscellaneous metabolites were annotated in the treated and non-treated plants.

As reported in the score plots (Fig. 5a, c), the PCA, performed on the plants treated for 15 and 30 days, respectively, showed a clear separation among all treatments. The sample separation was achieved using the principal components (PCs), PC1 versus PC2, which explained a

Fig. 4 **a** Concentration of chlorophyll *a* (Chl *a*), **b** (Chl *b*) and **c** total Chl *a* + *b*, **d** Chl *a/b* ratio, **e** total carotenoid concentration (Car tot), and **f** flavonoid index in leaves of sweet basil (*Ocimum basilicum* L.) plants irrigated without the addition of NaCl for 15 [$C_{(T15)}$] or 30 days [$C_{(T30)}$], irrigated with 50 mM NaCl for 15 [$C_{(T15)}$ + NaCl] or 30 days [$C_{(T30)}$ + NaCl], irrigated without NaCl and grown together with $C_{(T15)}$ + NaCl plants (NaCl-S), and NaCl-S plants further irrigated with 50 mM NaCl for 15 days (NaCl-S + NaCl). Data (means ± SD, *n* = 3) were subjected to one-way ANOVA and bars not accompanied by the same letter in step 1 (white bars) or step 2 (grey bars) are significantly different at $P \leq 0.05$ after LSD test
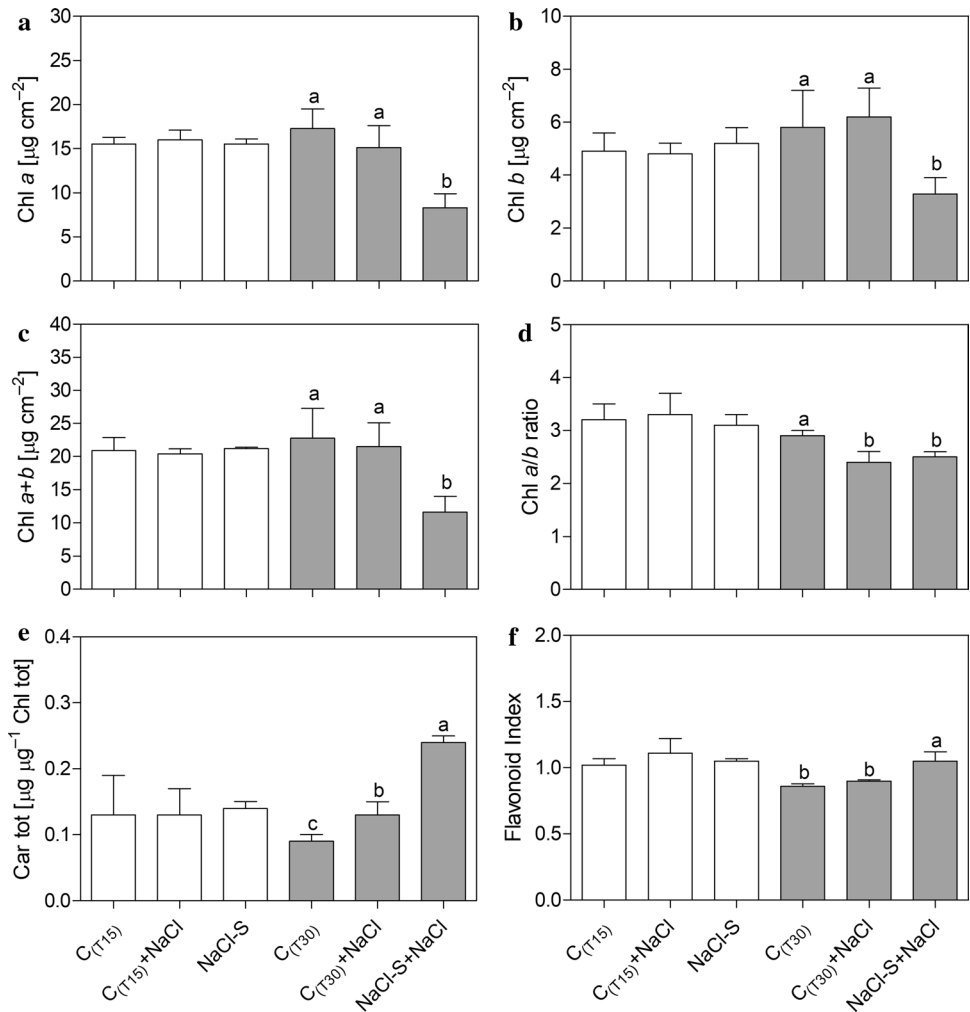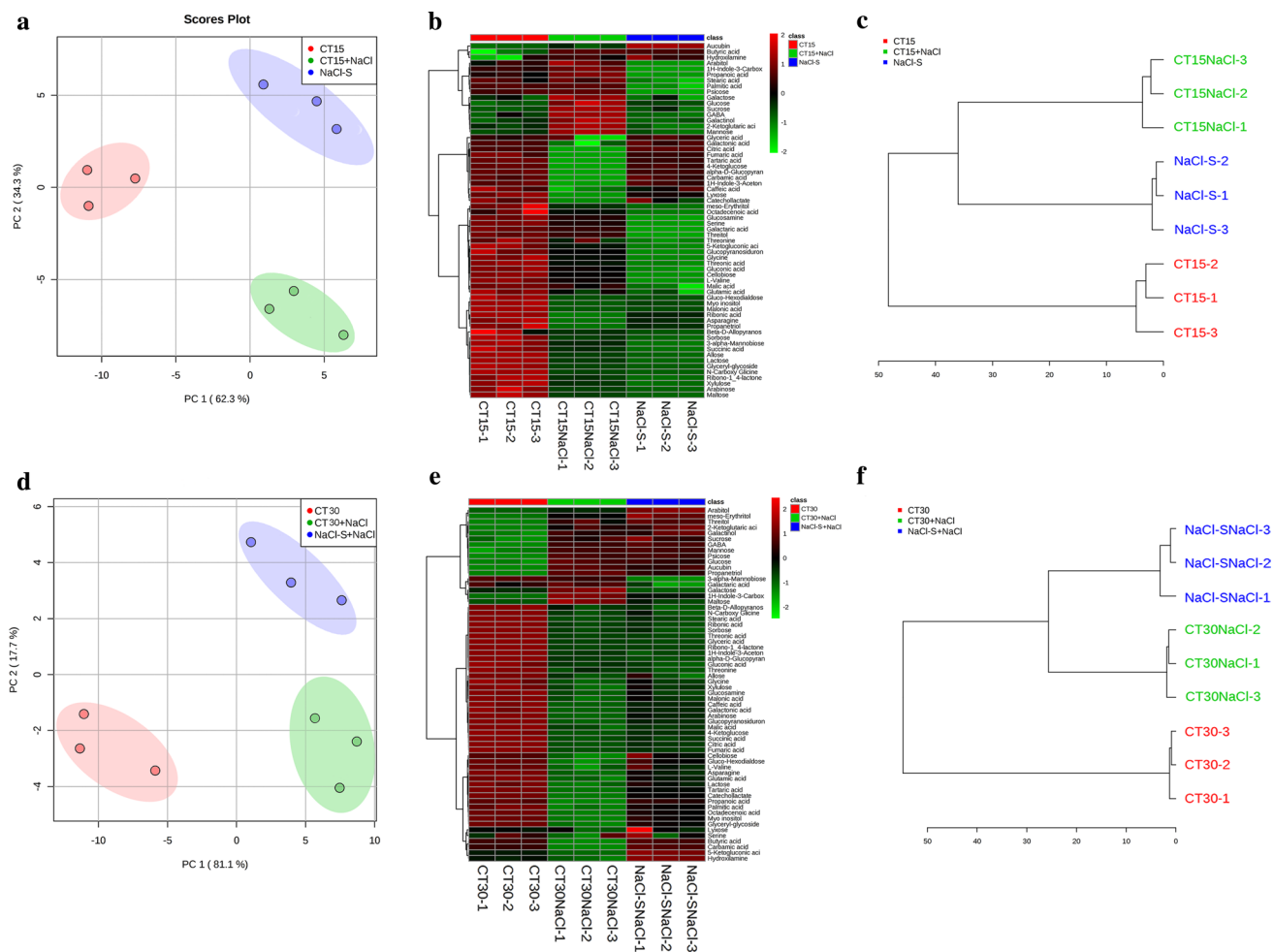
Fig. 5 Score plot of **a** the principal component analysis (PCA), **b** heat map, and **c** cluster analyses of the metabolite profiles of leaves of sweet basil (*Ocimum basilicum* L.) plants irrigated without the addition of NaCl for 15 days [$C_{(T15)}$], irrigated with 50 mM NaCl for 15 days [$C_{(T15)} + NaCl$], and irrigated without NaCl and grown together with $C_{(T15)} + NaCl$ plants. **d** Score plot of PCA, **e** heat map, and **f** cluster analyses of the metabolite profiles of leaves of sweet basil plants irrigated without the addition of NaCl for 30 days

[$C_{(T30)}$], irrigated with 50 mM NaCl for 15 days [$C_{(T30)} + NaCl$], exposed to $C_{(T15)} + NaCl$ plant volatiles and irrigated with 50 mM NaCl, namely NaCl-S + NaCl. For the heatmap, each square represents the effect of the treatment on the amount of each metabolite in an independent replicate using a false-color scale. Red or green regions indicate an increase or decrease metabolite content, respectively

total variance of 96.6% (PC1 = 62.3% and PC2 = 34.3%) in the plants treated for 15 days and 98.8% (PC1 = 81.1% and PC2 = 17.7%) in the plants treated for 30 days (Fig. 5a, c, respectively).

The PCA loading plots showed that after 15 days of treatment, PC1 was dominated largely by butyric acid, hydroxylamine, aucubin, lactulose, glucose, lactose, and malonic acid, and PC2 was dominated by carbamic acid, citric acid, 4-ketoglucose, and ^{1}H-indole-3-carboxaldehyde (Fig. S1a). In contrast, after 30 days of treatment, PC1 was mainly dominated by caffeic acid and glyceric acid, and PC2 was dominated by galactose, 3-α-mannobiose, 5-keto-gluconic acid gamma-lactone, butyric acid, and hydroxylamine (Fig. S1b). The heatmaps (Fig. 5b, d) only report annotated

metabolites and PCA, and highlight distinct segregation among the treatments.

Finally, the ANOVA analysis, performed at day 15 and day 30 separately, showed that 62 of 64 metabolites were substantially different among the treatments (Table S2).

VOC profile

As expected, in step 1, the volatilome profile revealed a strong difference among the control ($C_{(T15)}$) and salt-treated plants ($C_{(T15)} + NaCl$); however, the VOC profile of the receivers (NaCl-S) underwent considerable changes, as revealed by the heatmap (Fig. 6). When the VOC profiles of plants undergoing the treatment in step 1 were used for
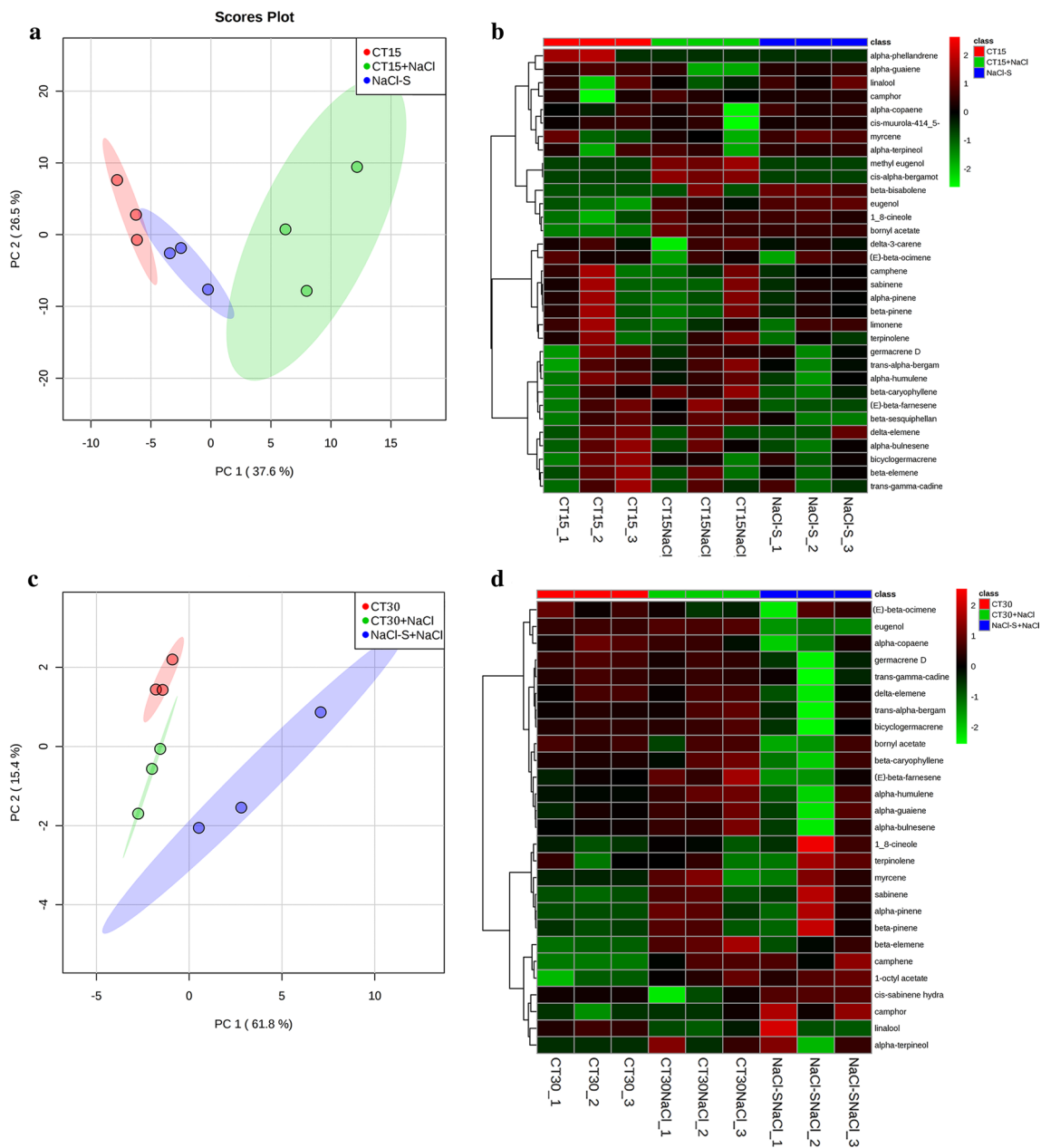
Fig. 6 **a** Score plot of the principal component analysis and **b** heat map derived from volatiles emitted by leaves of sweet basil (*Ocimum basilicum* L.) plants irrigated without the addition of NaCl for 15 days [$C_{(T15)}$], irrigated with 50 mM NaCl for 15 days [$C_{(T15)}$+NaCl], and irrigated without NaCl and grown together with $C_{(T15)}$+NaCl plants. **c** Score plot of the PCA and **d** heat map derived from volatiles emitted by the leaves of sweet basil plants irri- gated without the addition of NaCl for 30 days [$C_{(T30)}$], irrigated with 50 mM NaCl for 15 days [$C_{(T30)}$+NaCl], exposed to $C_{(T15)}$+NaCl plant volatiles and irrigated with 50 mM NaCl, namely NaCl-S+NaCl. For heatmap, each square represents the effect of the treatment on the amount of each metabolite in an independent replicate using a false-color scale. Red or green regions indicate an increase or decrease in the metabolite content, respectively

multivariate analyses, $C_{(T15)}$ and $C_{(T15)}$+NaCl plants were completely separated, whereas NaCl-S plants partially overlapped both controls and salt-treated plants in the score plot (Fig. 6a). PCA separation was achieved using PC1 versus PC2, which explained a total variance of 64.1%. In particular, PC1 explained 37.6% of the variance, while PC2 explained 26.5%. The PCA loading plot (Fig. S2a) shows

that PC1 was dominated largely by α-guaiene, *cis*-α-bergamotene, bornyl acetate, and methyl eugenol, and PC2 was dominated by α-terpineol, α-copaene, δ-3-carene, and *(E)*-β-ocimene.

The univariate analysis of data was performed to find the main significant differences in VOC profiles among the treatments, and the results from one-way ANOVA revealed five

VOCs, namely, *cis*-α-bergamotene, methyl eugenol, bornyl acetate, eugenol, and 1,8-cineole (Table S3; Table S4). All these volatiles were overproduced in $C_{(T15)} + NaCl$ plants, whereas bornyl acetate, eugenol, and 1,8-cineole were overproduced in salt-treated plants in comparison to $C_{(T15)}$ plants. NaCl-S plants had the highest production of eugenol among the treatments (Table S3).

In step 2, control ($C_{(T30)}$) and salt-treated plants ($C_{(T30)} + NaCl$) grouped again separately but the receivers of step 1 when treated with NaCl in step 2 (NaCl-S + NaCl) also grouped separately from the other two groups. The PC1 versus PC2 plot, used to achieve separation, explained 77.2% (PC1 = 61.8% and PC2 = 15.4%) of the total variance (Fig. 6c). The PCA loading plot highlighted that PC1 was mainly dominated by bicyclogermacrene, eugenol, germacrene D, and *trans*-γ-cadinene, and PC2 was dominated by 1-octyl-acetate, camphene, camphor, *(E)*-β-ocimene, and eugenol (Fig. S2b).

Four volatiles were differentially produced: eugenol, 1-octyl-acetate, β-elemene, and camphene (Tables S3). Compared with the $C_{(T30)}$ plants, $C_{(T30)} + NaCl$ plants, similar to $C_{(T15)} + NaCl$ plants in step 1, overproduced all these volatiles. NaCl-S + NaCl plants also overproduced all these volatiles except for eugenol, which accounted for the lowest produced volatile among the treatments.

Ethylene emission

Both $C_{(T15)} + NaCl$ and NaCl-S plants showed a higher level of ethylene emission, with the latter plants showing the highest values (+44% than $C_{(T15)}$ plants) (Fig. 7). In step 2, again salt treatment stimulated ethylene biosynthesis but compared with $C_{(T30)} + NaCl$ plants, the receiver plants had higher values of ethylene emissions when treated with NaCl.

Outdoor experiment in step 3

At the end of step 3, there were no differences in terms of total C among the treatments (Fig. 8a). The plants belonging to both salt treatments, i.e., $C_{(T65)} + NaCl$ and NaCl-S$_{(T65)} + NaCl$, had a higher C/N ratio and Na$^+$ and Cl$^-$ accumulation in their leaves compared with $C_{(T65)}$ plants (Fig. 8b–d, respectively). The receiver plants supplied with NaCl (NaCl-S$_{(T65)} + NaCl$) had the highest C/N ratio. Figure 8e, f shows the development of primordia in $C_{(T65)} + NaCl$ plants and the advanced flowering stage in NaCl-S$_{(T65)} + NaCl$ plants. Furthermore, NaCl-S$_{(T65)} + NaCl$ plants (Fig. 8f) produced a higher number of seeds than $C_{(T65)} + NaCl$ plants did (Fig. 8e). The number of seeds produced by $C_{(T65)}$ plants was higher than that by plants subjected to both treatments (208 ± 33), but for the purpose of the present experiment, the number of seeds is less relevant and is not discussed further.
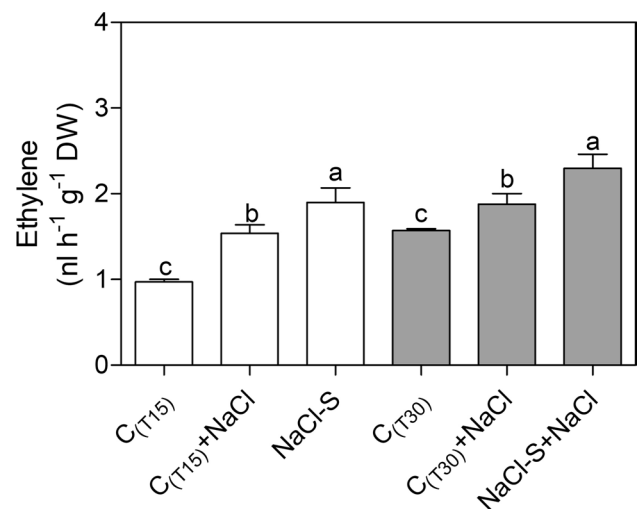
Fig. 7 Ethylene production in the leaves of sweet basil (*Ocimum basilicum* L.) plants irrigated without the addition of NaCl for 15 [$C_{(T15)}$] or 30 days [$C_{(T30)}$], irrigated with 50 mM NaCl for 15 [$C_{(T15)} + NaCl$] or 30 days [$C_{(T30)} + NaCl$], irrigated without NaCl and grown together with $C_{(T15)} + NaCl$ plants (NaCl-S), and NaCl-S plants further irrigated with 50 mM NaCl for 15 days (NaCl-S + NaCl). Data (means ± SD, $n = 3$) were subjected to one-way ANOVA, and bars not accompanied by the same letter in step 1 (white bars) or step 2 (grey bars) are significantly different at $P \leq 0.05$ after LSD test

Discussion

Besides conventional intraplant adaptive mechanisms, plants have also developed interplant communication through VOCs to share awareness of environmental stimuli. A considerable amount of literature exists on the ability of plants to alert neighboring plants when under attack by pathogens and/or herbivores; however, only a few reports have tested the possibility that abiotic stresses can similarly trigger plant–plant communication through volatiles. The only two reports available on plant–plant communication under salinity demonstrated that NaCl-treated plants of *Arabidopsis* (Lee and Seo 2014) and *V. faba* (Caparrotta et al. 2018) can alert neighboring plants against salinity, making the receivers less susceptible to salt-triggered damages. Even though results of the present experiment have to be carefully restricted to the experimental conditions applied therein, we offer for the first time the evidence that airborne signals emitted by salt-treated plants alert neighboring plants against salinity in a different way from the two aforementioned experiments, i.e. by promoting an earlier flowering in receivers, thus leading to higher seed production and an increased probability of their reproductive success. Beside possible ecological implication, we believe that such intraspecific communication has to be seriously considered when drawing an experimental design, especially in controlled conditions when plants belonging to different treatments are
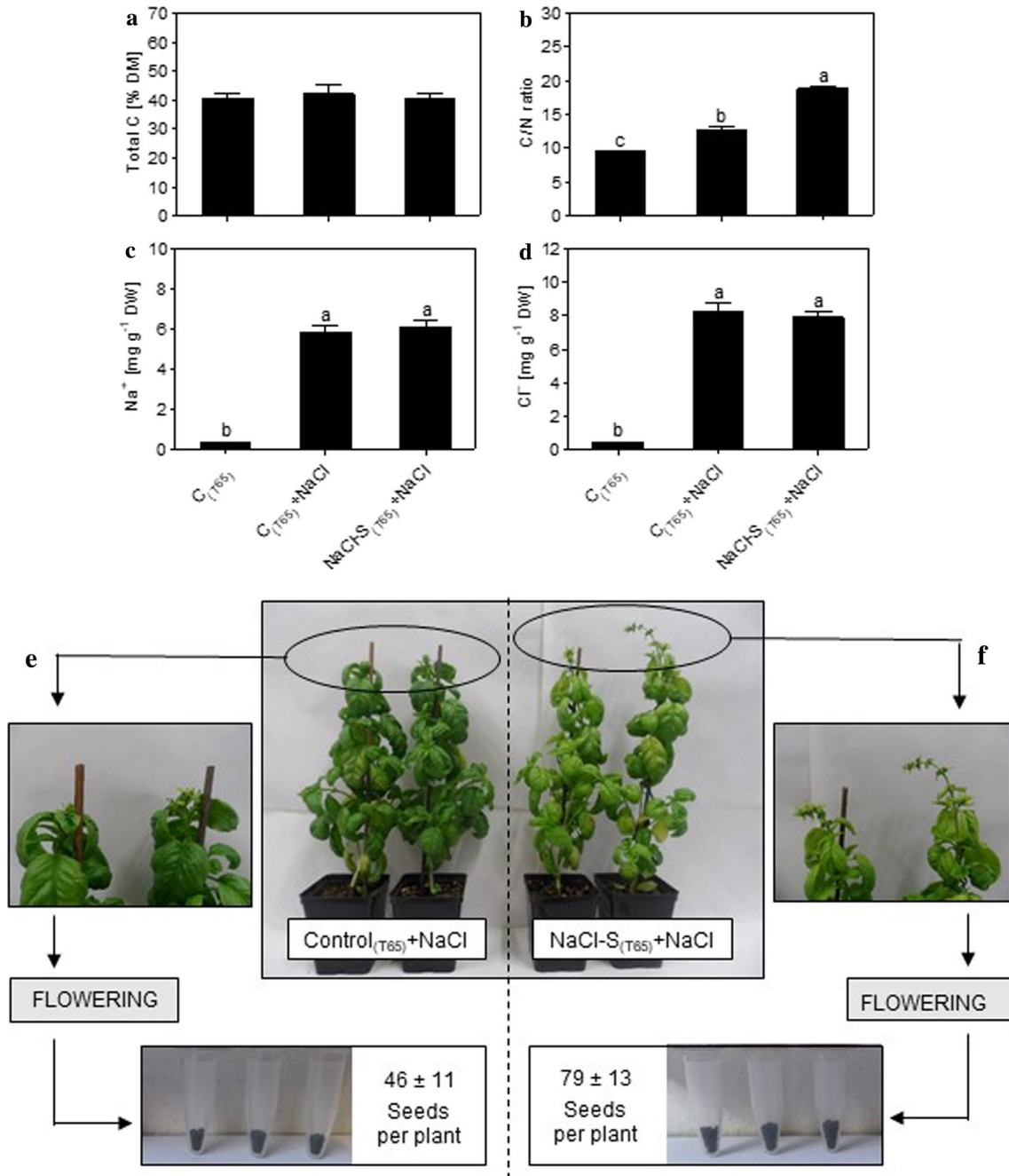
Fig. 8 **a** Percentage of total carbon, **b** carbon to nitrogen ratio (C/N), **c** concentration of Na$^+$ and **d** Cl$^-$ ions in control plants belonging to step 2 and further irrigated without the addition of NaCl for 35 days [C$_{(T65)}$], irrigated with 50 mM NaCl for 35 days [C$_{(T65)}$+NaCl], irrigated with 50 mM NaCl for 35 days and exposed in step 1 to airborne signals [NaCl-S$_{(T65)}$+NaCl]. For more details, see Material and method section. Data (means ± SD, $n=3$) were subjected to one-way ANOVA and bars not accompanied by the same letter in step 1 (white bars) or step 2 (grey bars) are significantly different at $P \leq 0.05$ after LSD test. Particulars of inflorescence and seed production in **e** C$_{(T65)}$+NaCl plants and f NaCl-S$_{(T65)}$+NaCl plants

not physically separated. We detail below the facets of this intriguing mechanism, which is further evidence of how plants are able to communicate with each other; however, we are unable to completely elaborate the mechanism.

Salinity-induced disturbances in plant metabolism have been exhaustively described. A hypersaline environment exerts two main effects on the growth and development of plants. First, such an environment causes water deficit in

plants as the roots are unable to extract water from the soil. Second, the hypersaline environment induces toxicity in plant tissues, where Cl^- and Na^+ ions excessively accumulate (Chaves et al. 2009; Shabala and Munns 2012). Under stress, plants can increase the fraction of carbon and the energy allocated to VOC production (Loreto and Schnitzler 2010; Loreto et al. 2014). The investment of carbon into VOCs can become a considerable sink for photochemical energy (Sharkey and Yeh 2001), which can explain the reduction of plant biomass, although similar values of A_N were observed in $C_{(T15)}+NaCl$ plants. In turn, neighboring unstressed plants perceive and promptly respond to such infochemicals, thus resulting in a fascinating web of ecological interactions (Dicke and Baldwin 2010) and on the possibility of receivers to "smell global climate change" (Yuan et al. 2009). However, the terms like "smelling" or "olfaction" have to be cautiously used when describing how plants detect VOCs, because there is little evidence that plants have a dedicated "olfactory system" like that in animals and, at present, a VOC receptor has only been described for ethylene (Cofer et al. 2018). Other physicochemical (e.g., changes of membrane gradient) and metabolic processes (e.g., reaction of emitter's VOCs with receiver's organic compounds) could be implicated in VOC detection and response (Matsui 2016), as, in most cases, compounds belonging to different chemical classes evoke a similar reaction in plants (Cofer et al. 2018). In our experiments, salinity promoted severe changes in the VOC fingerprint of $C_{(T15)}+NaCl$ plants, which influenced the behavior of companion unstressed plants, namely NaCl-S or receivers. Indeed, if the receiver plants did not differ in their shoot biomass or at the physiological level for most gas exchange parameters, a significant increment in WUE was one of the first physiological responses shown by the receivers to emitters' VOCs. In a similar experiment, Caparrotta et al. (2018) observed a more pronounced impairment of gas exchange parameters in receivers, especially in g_s reduction. The authors also observed that receivers had strongly constrained plant growth, similar to that detected in emitters. This difference is presumably dependent on the salt treatment imposed to emitters (150 mM NaCl), which was more severe than that used in the present experiment or perhaps to the higher responsiveness of *V. faba* than that of sweet basil plants to salinity.

The score plot of VOCs from step 1 plants showed strong differences between NaCl-S and $C_{(T15)}$ plants and revealed that the NaCl-S group partially overlapped with both $C_{(T15)}$ and $C_{(T15)}+NaCl$ groups. The heatmap of VOC biosynthesis in step 1 presents further clear evidence of the severe perturbation of receiver metabolism. Among the five VOCs, bornyl acetate and eugenol are key volatiles overproduced by sweet basil when supplied with 50 mM NaCl (Tarchoune et al. 2013), the same salt level that was used in the present study. In addition, both volatiles are involved in sharing the

awareness of biotic stress and/or pathogen attack among plants (Qualley and Dudareva 2001; Rai et al. 2004; Lusebrink et al. 2011; Dudareva et al. 2013). Considering the profile of VOCs produced by the plants grown in step 1, we could not attribute a definite role to any of these compounds. Notably, eugenol was also overproduced by the receivers, NaCl-S, compared with the emitters, $C_{(T15)}+NaCl$. In some cases, the overproduction of volatiles, under abiotic stress, depends on the plant developmental stage. Therefore, the profile of VOCs of salt-treated plants ($C_{(T30)}+NaCl$) in step 2, which were 15 days older than plants in step 1, might be helpful in discriminating salt-promoted age-dependent VOCs.

In step 2, eugenol was again overproduced by $C_{(T30)}+NaCl$ plants; thus, our hypothesis that eugenol is a key compound partially responsible for the induction of reactions in receiver plants becomes more realistic. However, our assumption deserves further investigation because (1) the receptors for most VOCs are not yet described in plants (Baldwin 2010) and (2) in many cases, based on the relative abundance of VOCs, plants react to a combination of VOCs (Matsui 2016) rather than to a single or a few VOCs.

Metabolomic analyses indicated severe salinity-induced disturbances in plant metabolism (see $C_{(T15)}+NaCl$, $C_{(T30)}+NaCl$, and NaCl-S+NaCl plants against their controls). All salt-treated plants showed an increase in sugars (sensu lato including polyalcohols), such as galactinol, galactose, mannose, glucose, and sucrose in response to salt stress, which can serve as osmoprotectants and as a carbon sink in plants subjected to salt stress (Urano et al. 2009; Singh et al. 2015). Beside the effect of ontogenesis which led to a reduced amount of amino acid even in t15 versus t30 plants, in salt-treated plants, amino acid, and organic acid contents were further reduced. Similar NaCl-promoted amino acid decline was previously observed in wheat and alfalfa treated with NaCl (Fougere et al. 1991; El-Bassiouny and Bekheta 2005).

Among the amino acids, γ-aminobutyric acid (GABA) was the only amino acid for which an increase was observed in emitters but not in receivers. One of the first responses induced by salinity in plants includes the stimulation of GABA biosynthesis (Bolarín et al. 1995), which plays several roles in plant response to abiotic stresses, such as nitrogen storage regulation (Breitkreuz et al. 1999), cytosolic pH regulation (Shelp et al. 1999), oxidative stress protection (Bouché et al. 2003a), and osmoregulation (Kinnersley and Turano 2000; Bouché et al. 2003b). The increase in GABA content might also be associated with ethylene overproduction through enhanced aminocyclopropane-1-carboxylic acid synthase activity (Kathiresan et al. 1997), which synergistically increases the production of other VOCs (Ruther and Kleier 2005). The plants exposed to stresses showed altered VOC blends and increased ethylene production. These

results suggest a possible interconnection between GABA, VOC, and ethylene accumulation under stress salinity.

Ethylene itself might therefore be another potential candidate explaining the plant–plant communication of salt stress and might have a direct role through its detection by receiver-dedicated receptors, and/or play a role in the transduction pathway underlying plant response to some terpenes, as observed for other phytohormones (Erb 2018). Understanding the involvement of ethylene in future experiments is of crucial importance to have a clear conclusion. If ethylene would have a direct action, NaCl-S + NaCl plants, which produced a higher level of ethylene than controls (but not of eugenol), would have maintained the capacity to "forward" the message to neighboring plants, and possibly to amplify the message, given that NaCl-S + NaCl plants produced ~ 18% more ethylene than $C_{(T30)}$ + NaCl plants did.

Along with more ethylene release, NaCl-S + NaCl plants showed typical traits of early senescence, such as severe alteration of photosynthetic parameters (F_v/F_m, A_N, and intercellular CO_2 concentration C_i), reduction in chlorophyll concentration associated with increased carotenoid and flavonoid levels, higher C/N ratio, and fluctuation of targeted metabolites, compared with $C_{(T30)}$ + NaCl plants. Among the plant metabolites, high sugar levels may also increase ethylene release or ethylene sensitivity by the plants and act as a senescence enhancer (Hoeberichts et al. 2007). Similarly, GABA levels might increase strongly during leaf senescence (Lähdesmäki 1968; Masclaux et al. 2000), since GABA amplifies stress signals by increasing ethylene synthesis (Kinnersley and Turano 2000). Generally, early senescence is considered as a negative aspect, but early senescence in our experiments boosted the flowering stage and the reproductive cycle of the salt-treated receiver plants (see Fig. 8e, f). This allowed NaCl-S + NaCl plants to produce a significantly higher number of seeds per plant compared with $C_{(T30)}$ + NaCl plants at the end of their reproductive cycle. Beside this difference, both NaCl-S + NaCl and $C_{(T30)}$ + NaCl plants showed an earlier flowering than $C_{(T30)}$ plants (data not shown), which is supportive for a salt-promoted effect on flowering stage. Although the observed increase in the reproductive success of salt-treated receivers in this study (the germination rate of seeds of salt-treated emitters was also similar to that of salt-treated receivers; data not shown) the two main factors on which the increase might be dependent deserve future investigation. First, the higher yield might be dependent on the lower Na^+ and Cl^- uptake by the receiver plants at the end of their cycle, given that $C_{(T65)}$ + NaCl and NaCl-S$_{(T65)}$ + NaCl had similar levels of both ions, but the latter plants concluded their cycle 15–20 days earlier. Second, changes in the VOC profiles observed between salt-treated emitters and receivers may have reduced the visit of pollinators, as supported by recent studies that demonstrated that changes in VOC emissions can negatively affect pollinator attraction (Kessler et al. 2011; Pareja et al. 2012).

Conclusion

The obtained results offer new evidence of how intraspecific communication in plants is crucial for sharing awareness of abiotic stresses. The results also reveal that priming by emitters does not offer a direct advantage to the physiological performance of receivers but increases their reproductive success. We are aware that some specific aspects need to be clarified in future experiments. First, the intimal connection among VOC perception, signaling transmission, and activation of biochemical/molecular reactions through which receivers accommodate salt stress needs a thorough investigation. In addition, although most studies of plant–plant communication sacrifice ecological realism to increase the likelihood of obtaining a response, we believe that our results have to be examined under more realistic conditions to validate our results in a broader context of plant ecology. The volatile-triggered communication, conversely, should be more seriously considered when performing the experiments in controlled conditions where control and treated plants are not physically separated, e.g., in greenhouses or growth chambers.

Author contribution statement ML experimental design, physiological and biochemical analyses, data acquisition, writing original draft; FA metabolomics analyses, data curation, review and editing; GF volatile determination, data curation, review and editing; ELP physiological analyses, review and editing; AT ethylene determination, data curation, review and editing; MRA review and editing; LG conceptualization, founding acquisition, final review and editing.

References

Adams RP (1995) Identification of essential oil components by gas cromatography and mass spectroscopy. Allured Publishing Corp, Illinois

Agati G, Cerovic ZG, Pinelli P, Tattini M (2011) Light-induced accumulation of *ortho*-dihydroxylated flavonoids as non-destructively monitored by chlorophyll fluorescence excitation techniques. Environ Exp Bot 73:3–9

Ameye M, Allmann S, Verwaeren J, Smagghe G, Haesaert G, Schuurink RC, Audenaert K (2017) Green leaf volatile production by plants: a meta-analysis. New Phytol 220:666–683

Araniti F, Lupini A, Sunseri F, Abenavoli MR (2017) Allelopathic potential of Dittrichia voscosa (L.) W. Greuter mediated by VOCs: a physiologycal and metabolomic approach. PLoS One 12:e0170161

Baldwin IT (2010) Plant volatiles. Curr Biol 20:392–397

Baldwin IT, Schultz JC (1983) Rapid changes in tree leaf chemistry induced by damage: evidence for communication between plants. Sci 221:277–279

Bibbiani S, Colzi I, Taiti C, Guidi Nissim W, Papini A, Mancuso S, Gonnelli C (2018) Smelling the metal: volatile organic compound emission under Zn excess in the mint Tetradenia riparia. Plant Sci 271:1–8

Bolarín MC, Santa-Cruz A, Cayuela E, Pérez-Alfocea F (1995) Short-term solute changes in leaves and roots of cultivated and wild tomato seedlings under salinity. J Plant Physiol 147:463–468

Bouché N, Fait A, Bouchez D, Moller SG, Fromm H (2003a) Mitochondrial succinic-semialdehyde dehydrogenase of the γ-aminobutyrate shunt is required to restrict levels of reactive oxygen intermediates in plants. Proc Nat Acad Sci USA 100:6843–6848

Bouché N, Lacombe B, Fromm H (2003b) GABA signaling: a conserved and ubiquitous mechanism. Trends Cell Biol 13:607–610

Breitkreuz KE, Shelp BJ, Fischer WN, Schwacke R, Rentsch D (1999) Identification and characterization of GABA, proline and quaternary ammonium compound transporters from Arabidopsis thaliana. FEBS Lett 450:280–284

Caparrotta S, Boni S, Taiti C, Palm E, Mancuso S, Pandolfi C (2018) Induction of priming by salt stress in neighboring plants. Environ Exp Bot 147:261–270

Catola S, Centritto M, Cascone P, Ranieri A, Loreto F, Calamai L, Balestrini R, Guerrieri E (2018) Effects of single or combined water deficit and aphid attack on tomato volatile organic compound (VOC) emission and plant–plant communication. Environ Exp Bot 153:54–62

Ceccanti C, Landi M, Benvenuti S, Pardossi A, Guidi L (2018) Mediterranean wild edible plants: weeds or "new functional crops"? Molecules 23:2299

Chaves MM, Flexas J, Pinheiro C (2009) Photosynthesis under drought and salt stress: regulation mechanisms from whole plant to cell. Ann Bot 103:551–560

Cofer TM, Seidl-Adams I, Tumlinson JH (2018) From acetoin to (Z)-3-hexen-1-ol: the diversity of volatile organic compounds that induce plant responses. J Agric Food Chem 66:11197–11208

Covarrubias AA, Cuevas-Velazquez CL, Romero-Pérez PS, Rendón-Luna DF, Chater CCC (2017) Structural disorder in plant proteins: where plasticity meets sessility. Cell Mol Life Sci 74:3119–3147

Dicke M, Baldwin IT (2010) The evolutionary context for herbivore-induced plant volatiles: beyond the 'cry for help'. Trends Plant Sci 15:167–175

Dudareva N, Klempien A, Muhlemann JK, Kaplan I (2013) Biosynthesis, function and metabolic engineering of plant volatile organic compounds. New Phytol 198:16–32

El-Bassiouny HM, Bekheta MA (2005) Effect of salt stress on relative water content, lipid peroxidation, polyamines amino acids and ethylene of two wheat cultivars. Int J Agric Biol 7:363–368

Erb M (2018) Volatiles as inducers and suppressors of plant defense and immunity-origins, specificity, perception and signaling. Curr Opin Plant Biol 44:117–121

Fincheira P, Quiroz A (2018) Microbial volatiles as plant growth inducers. Microbiol Res 208:63–75

Forieri I, Hildebrandt U, Rostas M (2016) Salinity stress effects on direct and indirect defence metabolites in maize. Environ Exp Bot 122:68–77

Fougere F, Le Rudulier D, Streeter JG (1991) Effects of salt stress on amino acid, organic acid and carbohydrate composition of roots, bacteroids, and cytosol of alfa alfa (Medicago sativa L.). Plant Physiol 96:1228–1236

Goulas Y, Cerovic ZG, Cartelat A, Moya I (2004) Dualex: a new instrument for field measurements of epidermal ultraviolet absorbance by chlorophyll fluorescence. Appl Opt 43:4488–4496

Guerrieri E (2016) Who's listening to talking plants? In: Ginwood R, Blande J (eds) Deciphering chemical language of plant communication. Signaling and communication in plants series. Springer, Basel, pp 117–136

Hoeberichts FA, Van Doorn WG, Vorst O, Hall RD, Van Wordragen MF (2007) Sucrose prevents up-regulation of senescence-associated genes in carnation petals. J Exp Bot 58:2873–2885

Jalali F, Zafari D, Salari H (2017) Volatile organic compounds of some Trichoderma spp. increase growth and induce salt tolerance in Arabidopsis thaliana. Fungal Ecol 29:67–75

Jones JB (1998) Plant nutrition manual. CRC Press, Boca Raton

Kathiresan A, Tung P, Chinnappa CC, Reid DM (1997) Gamma-aminobutyric acid stimulates ethylene biosynthesis in sunflower. Plant Physiol 115:129–135

Kegge W, Pierik R (2010) Biogenic volatile organic compounds and plant competition. Trends Plant Sci 15:126–132

Kessler A, Halitschke R, Poveda K (2011) Herbivory-mediated pollinator limitation: negative impacts of induced volatiles on plant–pollinator interactions. Ecology 92:1769–1780

Kinnersley AM, Turano FJ (2000) Gamma aminobutyric acid (GABA) and plant responses to stress. Crit Rev Plant Sci 19:479–509

Lähdesmäki P (1968) The amount of γ-amino butyric acid and the activity of glutamic decarboxylase in aging leaves. Physiol Plant 21:1322–1327

Landi M, Remorini D, Pardossi A, Guidi L (2013) Sweet basil (Ocimum basilicum) with green or purple leaves: which differences occur in photosynthesis under boron toxicity? J Plant Nutr Soil Sci 176:942–951

Lee K, Seo PJ (2014) Airborne signals from salt-stressed Arabidopsis plants trigger salinity tolerance in neighboring plants. Plant Signal Behav 9:e28392

Lichtenthaler HK, Buschmann C (2001) Chlorophylls and carotenoids: measurement and characterization by UV–Vis spectroscopy. Curr Prot Food Anal Chem 1:F4–8

Loreto F, Schnitzler JP (2010) Abiotic stresses and induced BVOCs. Trends Plant Sci 15:154–166

Loreto F, Dicke M, Schnitzler JP, Turlings TCJ (2014) Plant volatiles and the environment. Plant Cell Environ 37:1905–1908

Lusebrink I, Evenden ML, Blanchet FG, Cooke JEK, Erbilgin N (2011) Effect of water stress and fungal inoculation on monoterpene emission from an historical and a new pine host of the mountain pine beetle. J Chem Ecol 37:1013–1026

Masclaux C, Valadier MH, Brugière N, Morot-Gaudry JF, Hirel B (2000) Characterization of the sink/source transition in tobacco (Nicotiana tabacum L.) shoots in relation to nitrogen management and leaf senescence. Planta 211:510–518

Matsui K (2016) A portion of plant airborne communication is endorsed by uptake and metabolism of volatile organic compounds. Curr Opin Plant Biol 32:24–30

Papadakis IE, Tsiantas PI, Tsaniklidis G, Landi M, Psychoyou M, Fasseas C (2018) Changes in sugar metabolism associated to stem bark thickening partially assist young tissues of Eriobotrya japonica seedlings under boron stress. J Plant Physiol 231:337–345

Pardossi A, Romani M, Carmassi G, Guidi L, Landi M, Incrocci L, Maggini R, Puccinelli M, Vacca W, Ziliani M (2015) Boron accumulation and tolerance in sweet basil (Ocimum basilicum L.) with green or purple leaves. Plant Soil 395:375–389

Pareja M, Qvarfordt E, Webster B, Mayon P, Pickett J, Birkett M, Glinwood R (2012) Herbivory by a phloem-feeding insect inhibits floral volatile production. PLoS One 7:e31971

Pompeiano A, Landi M, Meloni G, Vita F, Guglielminetti L, Guidi L (2017) Allocation pattern, ion partitioning, and chlorophyll *a* fluorescence in *Arundo donax* L. in responses to salinity stress. Plant Biosyst 151:613–622

Qualley A, Dudareva N (2001) Plant volatiles. Wiley, Chichester

Rai V, Vajpayee P, Singh SN, Mehrotra S (2004) Effect of chromium accumulation on photosynthetic pigments, oxidative stress defense system, nitrate reduction, proline level and eugenol content of *Ocimum tenuiflorum* L. Plant Sci 167:1159–1169

Ruther J, Kleier S (2005) Plant–plant signaling: ethylene synergizes volatile emission in *Zea mays* induced by exposure to (Z)-3-hexen-1-ol. J Chem Ecol 31:2217–2222

Shabala S, Munns R (2012) Salinity stress: Physiological constraints and adaptive mechanisms. In: Shabala S (ed) Plant stress physiology. CAB International, Oxford, pp 59–93

Sharkey TD, Yeh S (2001) Isoprene emission from plants. Annu Rev Plant Physiol Plant Mol Biol 52:407–436

Shelp BJ, Bown AW, McLean MD (1999) Metabolism and functions of gamma-aminobutyric acid. Trends Plant Sci 4:446–452

Sims JT, Kline JS (1991) Chemical fractionation and plant uptake of heavy metals in soils amended with co-composted sewage sludge. J Environ Qual 20:387–395

Singh M, Kumar J, Singh S, Singh VP, Prasad SM (2015) Roles of osmoprotectants in improving salinity and drought tolerance in plants: a review. Rev Environ Sci Biotech 14:407–426

Tarchoune I, Baâtour O, Harrathi J, Cioni PL, Lachaâl M, Flamini G, Ouerghi Z (2013) Essential oil and volatile emissions of basil (*Ocimum basilicum*) leaves exposed to NaCl or Na_2SO_4 salinity. J Plant Nutr Soil Sci 176:748–755

Urano K, Maruyama K, Ogata Y et al (2009) Characterization of the ABA-regulated global responses to dehydration in *Arabidopsis* by metabolomics. Plant J 57:1065–1078

Xia J, Sinelnikov IV, Han B, Wishart DS (2015) MetaboAnalyst 3.0—making metabolomics more meaningful. Nucleic Acids Res 43:251–257

Yoneya K, Takabayashi J (2014) Plant–plant communication mediated by airborne signals: ecological and plant physiological perspectives. Plant Biotechnol 31:409–416

Yuan JS, Himanen SJ, Holopainen JK, Chen F, Stewart CN (2009) Smelling global climate change: mitigation of function for plant volatile organic compounds. Trends Ecol Evol 24:323–331